The College of Engineering
University of Wisconsin-Madison

Wisconsin Electric Machines and Power Electronics Consortium

RESEARCH REPORT
88-5

A Direct Field Oriented Controller for Induction Motor Drives Using Tapped Stator Windings

D. Zinger, F. Profumo, T.A. Lipo, and D.W. Novotny
Dept. of Electrical & Computer Engrg.
University of Wisconsin-Madison
1415 Johnson Drive
Madison, WI 53706-1691

WEMPEC

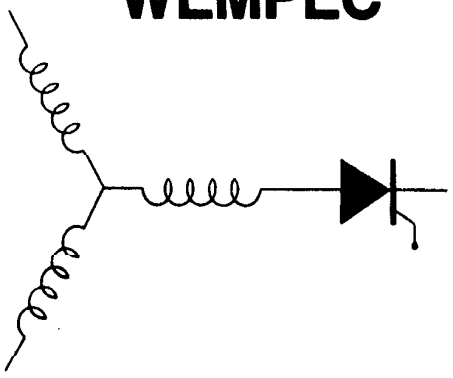

Department of Electrical and Computer Engineering
1415 Johnson Drive
Madison, Wisconsin 53706

A DIRECT FIELD ORIENTED CONTROLLER FOR INDUCTION MOTOR DRIVES USING TAPPED STATOR WINDINGS

D. Zinger, F. Profumo, T.A. Lipo and D.W. Novotny
University of Wisconsin
Department of Electrical and Computer Engineering
1415 Johnson Drive
Madison, WI 53706 U.S.A.

ABSTRACT

A direct method of field orientation has been implemented which requires little knowledge of machine parameters and which uses only readily measureable quantities. The system uses tapped stator windings to measure the air gap flux. The signals from the tapped windings are also used in a flux regulation loop. A speed controller is implemented using the ripples created in the tapped windings by the motion of the rotor slots through the flux for speed information.

INTRODUCTION

Significant advances in control hardware for ac adjustable speed induction motor drives has resulted in drives with excellent torque response. During this intense development period, enormous effort has been expended on improving indirect field oriented control by design of complicated controllers for compensating non ideal machine behavior such as parameter variations due to the temperature and/or magnetic saturation. Relatively little effort has been directed toward the design of other drive control structures which still exploit the motor capabilities but, in addition, also optimize hardware and software costs.

While the indirect method is highly dependent on motor parameters and requires the use of shaft encoders, the direct method has only a minimal dependency on motor parameters. By using tapped windings the necessary flux measurements can be made highly reliable. The direct field oriented control of an induction motor is thus a more straightforward method for designing a drive which does not require a continuous torque at zero speed. The system employs, in principle, a simple control structure which is less sensitive to changes in machine parameters over a wide range of operating conditions. The traditional approach of direct field oriented control with search coils or Hall effect sensors for flux sensing, however, introduces limitations due to machine structural and the thermal requirements. One solution to this problem is the design of a drive utilizing a machine in which the air gap flux is measured using taps that are part of the motor coils themselves[1]. This method also permits the use of an easily designed "PD feedback controller" by making use of the air gap flux together with the derivative of the air gap flux[2].

For implementation of a speed control at low cost it is mandatory to design a drive without a shaft encoder or other type of external speed sensor. In previous papers, a speed controller based on the calculation of the frequency of the rotor flux disregarding any slip compensation was developed. For this purpose a simple mathematical calculation was performed utilizing the calculated rotor flux of the machine and its derivative[2]. Unfortunately this method is unable to detect changes in slip due to load variations. The rotor speed can, therefore, vary significantly. Because of this limitation, speed regulation becomes relatively poor. This paper presents a new method for speed regulation which uses the rotor slot ripple detected from the voltages measured with the tapped stator windings. The overall solution then becomes a more optimum match between the components of the drive without overloading the control with heavy calculation and/or increasing the hardware significantly in comparison with traditional open loop adjustable speed drives.

DIRECT FIELD ORIENTATION USING FLUX SENSING

Tapped Winding Flux Sensing

The method for measuring flux utilizes voltages induced in the coils in two of the three motor phases[1]. The voltages are accessed by making available connection points within the motor as shown in Fig. 1. The voltage induced in each of two coils in the same phase is dependent on both the IR drop in the coil and flux passing through the coil i.e., that is:

$$v_1 = r\,i_1 + \frac{d\lambda_1}{dt} \tag{1}$$

$$v_2 = r\,i_2 + \frac{d\lambda_2}{dt} \tag{2}$$

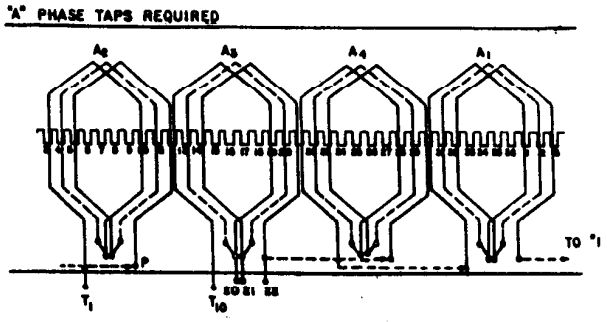

Fig. 1: Coil placement and taps on one phase of a double layer lap winding having 7 / 9 slot pitch.

Since two coils in the same phase have the same current and since they are wound similarly, they have the same resistance. By taking the voltage difference between two such coils the IR drop can be cancelled leaving only the difference between the flux derivatives, or

$$v_2 - v_1 = \frac{d(\lambda_2 - \lambda_1)}{dt} \tag{3}$$

It can be shown that the difference in flux voltages of two overlapping coils is, except for a small leakage, directly related to the airgap flux[3]. The d-q components of the airgap flux can be derived from voltages of the two phases using the equations :

$$\frac{d\lambda^s_{dm}}{dt} = k_1 \left[\int (v_{a1} - v_{a2})\, dt \right] \tag{4}$$

$$\frac{d\lambda^s_{qm}}{dt} = k_2 \left[2\int (v_{b1} - v_{b2})\, dt + \int (v_{a1} - v_{a2})\, dt \right] \tag{5}$$

where λ^s_{dm} is the d-component of the air gap flux in the stationary reference frame, λ^s_{qm} is the q-component of the air gap flux in the stationary reference frame, a_1 and a_2 are the coils related to phase a and b_1 and b_2 are the coils related to phase b.

Since for proper field orientation the system must be oriented with the rotor flux, a small conversion must be made to translate the measured airgap flux to the rotor flux. This can be accomplished using the equations :

$$\frac{d\lambda^s_{dr}}{dt} = \left(\frac{L_r}{L_m}\right)\frac{d\lambda^s_{dm}}{dt} - L_{lr}\frac{di^s_{ds}}{dt} \tag{6}$$

$$\frac{d\lambda^s_{qr}}{dt} = \left(\frac{L_r}{L_m}\right)\frac{d\lambda^s_{qm}}{dt} - L_{lr}\frac{di^s_{qs}}{dt} \tag{7}$$

where λ^s_{dr} is the d-component of the rotor flux in the stationary reference frame, λ^s_{qr} is the q-component of the rotor flux in the stationary reference frame, L_r is the rotor self inductance, L_m is the mutual inductance and L_{lr} is the rotor leakage.

Because of these relationships the measurement of rotor flux depends on motor parameters. The rotor leakage inductance (L_{lr}) is relatively constant, independent of temperature and flux level. It does, however, have some dependence on rotor current (and thus motor load) but this can be compensated if necessary. The ratio of rotor self inductance to mutual inductance (L_r/L_m) is nearly unity and changes only slightly with saturation. Once proper values in the flux relationships are established, therefore, there is little need for further parameter adjustments in most cases.

Flux PD Feedback Control

The field orientation technique requires that the current commands be oriented to the rotor flux. Errors in orientation may cause improper flux settings and consequent errors in electromagnetic torque. A fast acting flux regulator can usually compensate for such errors. In most regulating systems a PI (proportional-integral) controller is typically used. However, for the system considered here this approach would require an additional integration to calculate the flux from its derivatives, Eqs. 6 and 7. Since the derivative of the flux is available as a measured quantity rather than the flux itself it would be preferable to use this signal in a faster acting, PD or PID control scheme so that the cost of the two additional integrators can be dispensed with. Figure 2 shows the implementation of a control scheme using the flux and its derivative, a PD feedback arrangement.

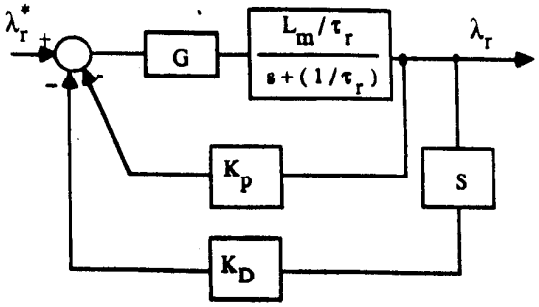

Fig. 2: Simplified flux control loop with PD feedback controller.

A comparison of these two control schemes can be made by introducing a step change in flux command. In Fig. 3 the magnitude of the rotor flux is shown related to the PD feedback controller for a step in flux command. The rise time can be observed to be about 180 msec. This compares favorably with the waveform in Fig. 4 which depicts the same response for a PI controller. The PD control, however, has some inherent problems. Noise and offsets in the feedback signal can be amplified by this control making it less attractive for applications in noisy environments.

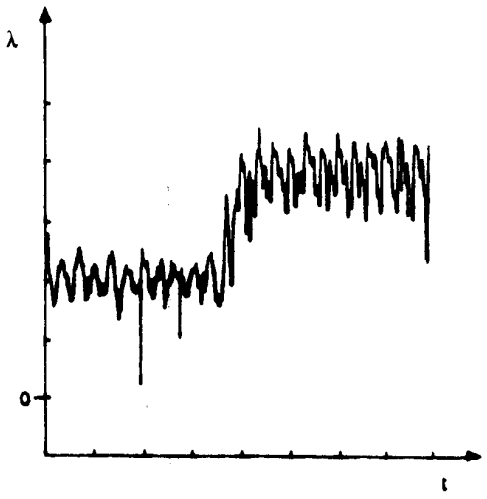

Fig. 3: Flux response to a step change in flux command with PD feedback controller. (Time scale 200 ms / div).

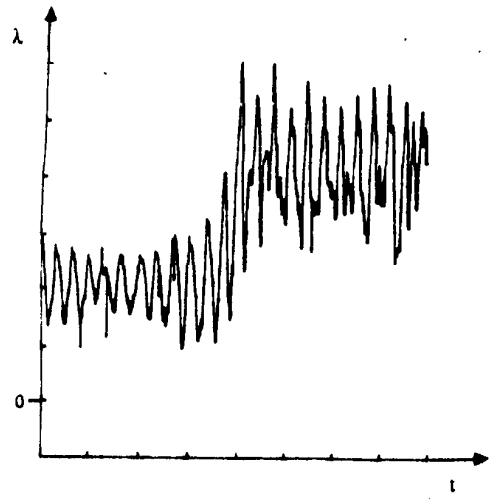

Fig. 4: Flux response to a step change in flux command with PI feedforward controller. (Time scale 200 ms/div).

METHOD FOR IMPROVING SPEED CONTROL

For the design of a low cost reliable drive the removal of the tachometer and other external position or speed sensor is typically mandatory. However, the design of a speed loop requires a signal proportional to the actual mechanical speed. By utilizing the voltages measured with the tapped stator windings, the rotor slot ripple can be detected for the purpose of calculating the slip [4]. The voltage induced by the air gap flux for each of the tapped winding coils can be written:

$$v(\theta,\omega t) = -B_0 k_{B1}\omega \sin(\omega t - \theta) - \frac{1}{2}B_0 k_n k_{B+}(N_r\omega_r+\omega)\sin\left[(N_r\omega_r+\omega)t - (N_r+1)\theta\right] - \frac{1}{2}B_0 k_n k_{B-}(N_r\omega_r-\omega)\sin\left[(N_r\omega_r-\omega)t - (N_r-1)\theta\right] \quad (8)$$

where

θ = electrical position with respect to the stator

ω_r = mechanical speed in electrical rad/sec

ω = supply frequency in electrical rad/sec

N_r = number of rotor slots per pole pair

B_0 = modulus of fundamental component of flux density

k_n = amplitude ratio (dependent on rotor current)

k_{Bx} = constant dependent on the coil configuration for a given harmonic

Isolation of Slot Harmonics

It is unfortunate that the fundamental component of Eq. (8) is considerably larger than the desired slot harmonics. To eliminate this component, the sum of voltages from three coils placed 120 electrical degrees apart can be taken. The effect of such a sum on any harmonic *h* can be written in the form :

$$v_h = k[\sin(A) + \sin(A - \frac{2\pi h}{3}) + \sin(A + \frac{2\pi h}{3})] \quad (9)$$

This equation has a zero value not only for the fundamental but for all values of *h* except integer multiples of three. Since *h* corresponds to N_r+1 for the upper slot harmonic and N_r-1 for the lower slot harmonic, and if the number of rotor slots is not a multiple of three, one and only one of the slot harmonics will remain. Motor design practice avoids rotor slot numbers which are multiples of three to reduce noise and vibration [5]. Thus, by summing the voltages in this manner only one slot harmonic remains together with other harmonics that are a multiple of three times the fundamental.

A spectrum of the voltage from the sum of three coils 120 electrical degrees out of phase is shown in Fig. 5. Along with the desired slot harmonic this spectrum shows a major third harmonic component. This third harmonic is the result of saturation and other imperfect conditions found in most induction machines. Because of this harmonic, further filtering is required to isolate the desired ripple. Since there is a wide range of desired frequencies of operation, a standard bandpass filter could not be employed. It becomes necessary to use a filter, such as a switched capacitor filter, whose center frequency is easily adjusted[6]. Since the fundamental frequency can be measured independently, the sampling rate of a switched capacitor filter can be adjusted to have a center frequency of $(N_r+1)\omega$ or $(N_r-1)\omega$ depending on the harmonic to be isolated. By choosing the proper bandwidth, the filter will eliminate the third harmonic while allowing the slot ripple to pass. The spectrum, shown in Fig. 6, of the voltage sum of three coils passed through such a filter demonstrates that the desired slot harmonic can be properly isolated by using this approach.

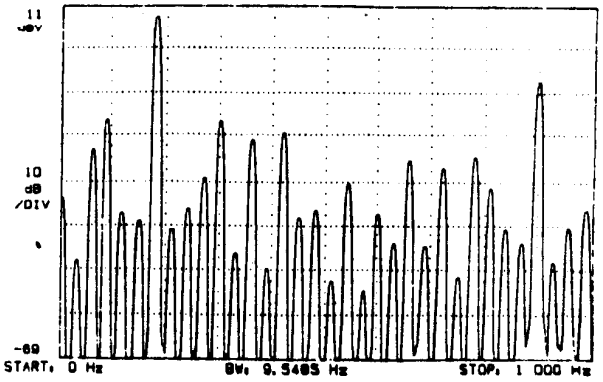

Fig. 5: Spectrum of flux voltages from sum of 3 tapped winding flux sensors.

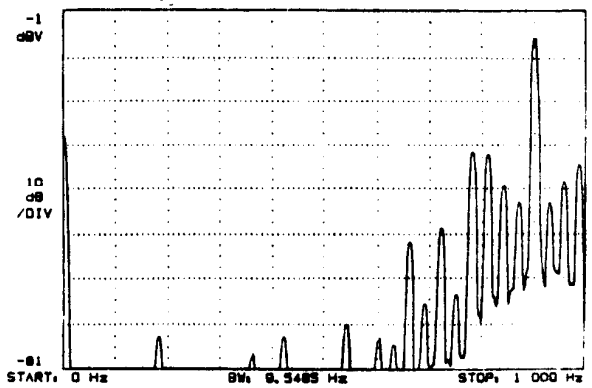

Fig. 6: Spectrum of flux voltages from sum of 3 tapped winding flux sensors after filtering.

Detection of Rotor Speed

Two methods of extracting rotor speed information from the properly isolated slot harmonic are indicated by Eq. (8). One possible method of detecting speed might be to use the magnitude of the harmonic since it is directly related to speed. Another method is to use the frequency of the harmonic which is also related to rotor speed.

The magnitude of the slot harmonic unfortunately depends not only on the rotor speed but also on other factors such as rotor current. Any magnitude speed detection scheme would, therefore, require adjustments dependent on operating conditions. Since the frequency is less dependent on other parameters, it is a better choice for speed control.

As a means to detect the frequency, a phase locked loop (PLL) was employed as shown in Fig. 7. Without any input voltage (V_S) the VCO (voltage controlled oscillator) will generate a frequency related to the base frequency input (V_f). When a slot frequency is applied at V_S the signal is multiplied by the VCO signal to create a beat frequency. If the VCO frequency and the slot frequency are sufficiently close, the beat frequency will be low enough to pass through the low pass filter and modify the VCO output. The VCO signal will continue to be modified until it locks onto the signal at V_f. The output voltage (V_{out}) is always directly related to the VCO frequency and, under these conditions, would be related to the frequency at V_f. By choosing a base frequency of $(N_r \pm 1)\omega$ the initial signal from the VCO will differ by $N_r\omega_s$. This is a relatively low frequency if the system is to lock.

When the circuit is locked the system can be described by the linear system shown in Fig. 8. The transfer function for this system is described by :

$$\frac{\omega(s)}{\theta_r(s)} = \frac{s\,k_\phi\,k_f}{\tau s^2 + s + k_\phi\,k_f\,k_{vco}} \qquad (10)$$

where k_ϕ is the constant multiplier, k_f is the filter constant and k_{VCO} is the VCO constant

Hence, the system can be characterized as having a second order response. The system response to changes in frequency will, of course, depend on the parameter settings. The transient response depends on the choice of parameters, but when choosing these parameters the "lock in" capture frequency ranges must also be considered.

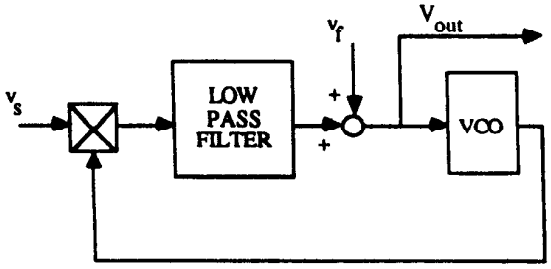

Fig. 7: Block diagram of Phase Locked Loop.

The lock-in range is the span of frequencies from the center frequency to the frequency where the PLL will remain locked after having been initially locked (see Fig. 9). This range can be shown to be in the region where the steady state phase error remains linear[7]. Often this range is taken to be ±1 radian to assure linearity. For the system described with the error taken at ±1 radian the lock in range ω_L can be defined as :

$$\omega_L = k_f\,k_\phi\,k_{vco} \qquad (11)$$

The capture range is the span of frequencies from the center frequency to the frequency where the system will initially lock (see Fig. 9). This is a transient condition which is difficult to calculate exactly. For the given system the capture range ω_C can be approximated by :

$$\omega_c \cong \sqrt{\frac{k_\phi\,k_f\,k_{vco}}{\tau}} \qquad (12)$$

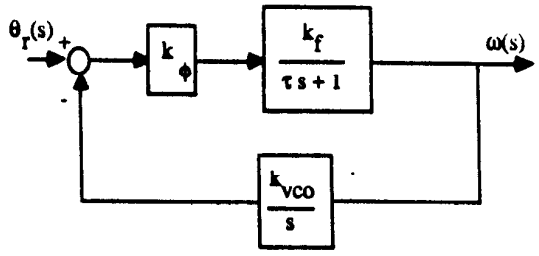

Fig. 8: Linearized equivalent Phase Locked Loop circuit.

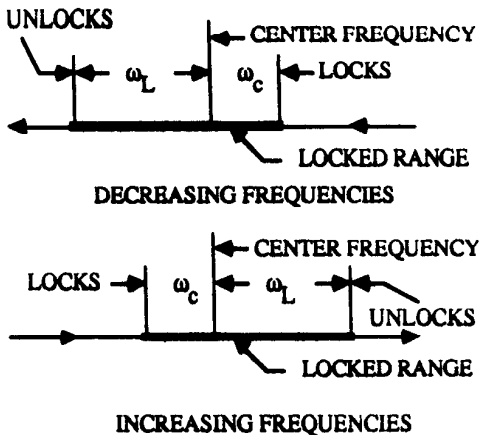

Fig. 9: Important frequencies for Phase Locked Loop.

Both the system natural frequency and damping are tied to these frequencies. The natural frequency ω_n is given by :

$$\omega_n = \sqrt{\frac{k_\phi k_f k_{vco}}{\tau}} = \omega_c \qquad (13)$$

and the damping ζ by :

$$\zeta = \frac{1}{2}\sqrt{\frac{1}{\tau k_\phi k_f k_{vco}}} = \frac{1}{2}\frac{\omega_c}{\omega_L} \qquad (14)$$

For the system under consideration the capture range is particularly important. It would be desirable to set the capture frequency to be not much larger than the largest possible slip component ($N_r \cdot \omega_{smax}$). This would allow locking on the slot harmonic without much of a possibility of locking on another signal. Choosing the capture frequency in this manner, however, limits the system bandwidth. In general, the bandwidth should be sufficiently wide to satisfy the dynamic requirements of the application.

The choice of a locking frequency is less critical than the choice of the capture frequency. Because the base frequency moves with synchronous speed, the frequency error should not be much larger than the slip. The locking frequency, therefore, need not be much larger than the capture frequency and can be chosen to be slightly larger than the capture frequency to assure the system remains locked during transients. However. some adjustment can be allowed to help achieve proper damping.

IMPLEMENTED SOLUTION

On the basis of the above considerations, a drive system with direct field orineted control has been implemented in the laboratory. In particular, a three phase induction motor with tapped stator windings has been utilized supplied by a current controlled PWM inverter that employs power transistors as its power switching devices. A pulse width wave form is generated from the differences between the current command and the actual waveform using a ramp comparator. The current command is computed from the flux voltages using the direct field oriented control method and has been implemented digitally in an INTEL 80286 microprocessor. Figure 10 shows a simplified block diagram of the overall system implementation. Some of the central functions implemented with the microprocessor are shown in Fig. 11.

EXPERIMENTAL RESULTS

To check for proper speed regulation, speed was measured as a function of applied torque and compared to the speed when the motor is operated with a regulated frequency source. At higher speeds, as shown in Fig. 12, there is considerable improvement in speed regulation until the voltage limit on the inverter causes a loss of current control. At lower speeds the voltage limit is not a factor and speed is regulated well up to the torque limits of the drive, as shown in Fig. 13. At even lower speeds,as shown in Fig. 14, speed regulation is again poor because the slot harmonic signal is reduced and harder to lock onto and also because phase errors introduced by filters in the system reduce the torque producing capabilities.

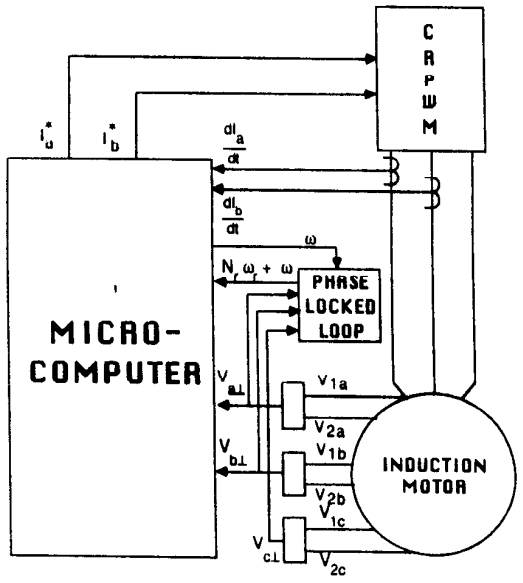

Fig. 10: Block diagram of overall system.

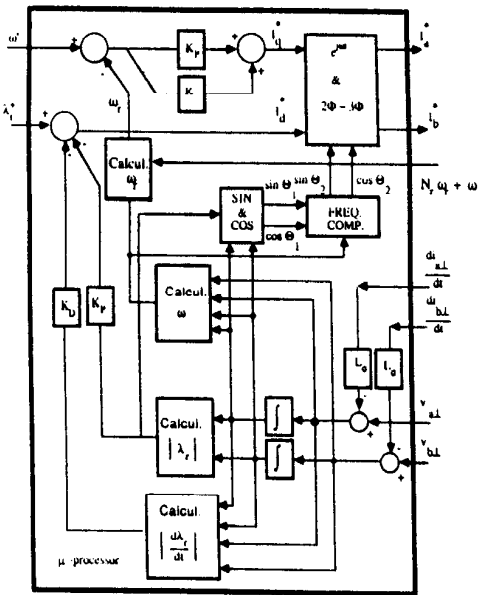

Fig. 11: Block diagram of microprocessor controller.

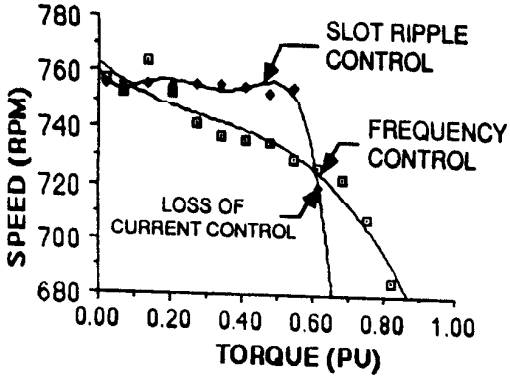

Fig. 12: Speed torque curves while running at approximately 25 Hz.

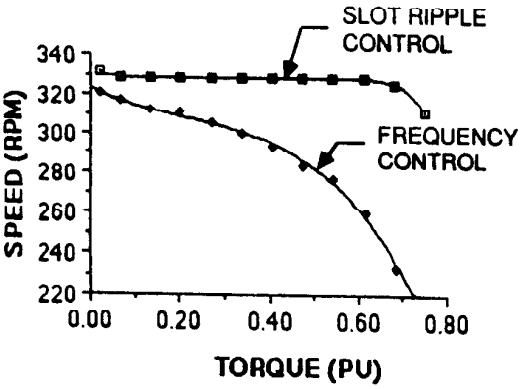

Fig. 13: Speed torque curves while running at approximately 10 Hz.

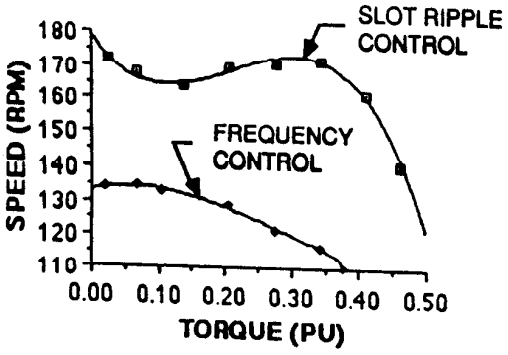

Fig. 14: Speed torque curves while running at approximately 5 Hz.

To check the speed regulator dynamic response, a step load of approximately half the rated torque was applied to the machine. A quick recovery was accomplished when operating at about 720 rpm as shown in Fig. 15. Although the regulation was not as good when operating at 120 rpm, the recovery time for the transient could still be considered acceptable as seen in Fig. 16.

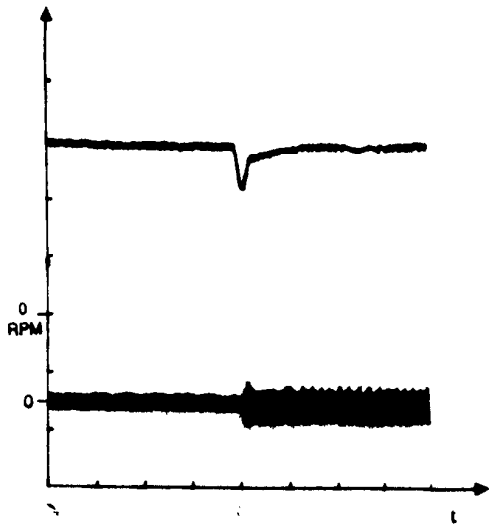

Fig. 15: Speed response to 0.5 step in torque with commanded speed 720 rpm. Top trace:Speed: (226 rpm/div) Bottom trace: Current : (10 amp/div) Time scale: 1 sec / div.

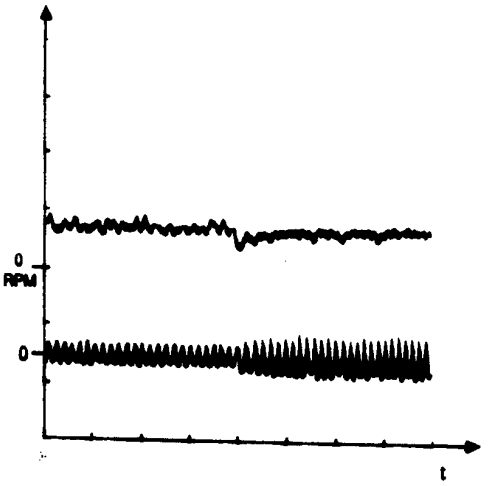

Fig. 16: Speed response to 0.5 step in torque with commanded speed 1200 rpm. Top trace: Speed (226 rpm/div) Bottom trace: Current (10 amp/div) Time scale: 1 sec/div.

A further check of the dynamics of the system was done by giving step changes in speed command under different loading conditions. For no load conditions a step increase in speed command is shown in Fig. 17 and a step decrease in speed is shown in Fig. 18 . For both cases the response was fast but there was considerable overshoot. This response occurs because the parameters in the control loop were chosen to compromise speed command performance in exchange for an improved response to a load disturbance. The step increase and decrease in speed for loaded conditions is shown in Fig. 19 and 20 respectively. The load consisted of a torque proportional to speed such that at the top speed (approximately 600 rpm) the motor was operating at 50% torque. Because of the damping effect of the load, the response slowed slightly and the overshoot was reduced.

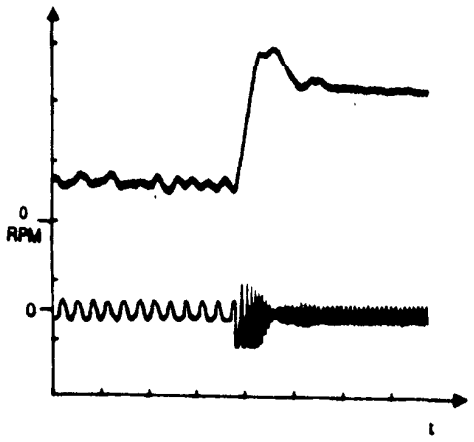

Fig. 17: Respose to step in speed command from 120 to 600 rpm at no load. Top trace: Speed (226 rpm/div) Bottom trace: Current (10 amp/div). Time scale: 500 ms/div.

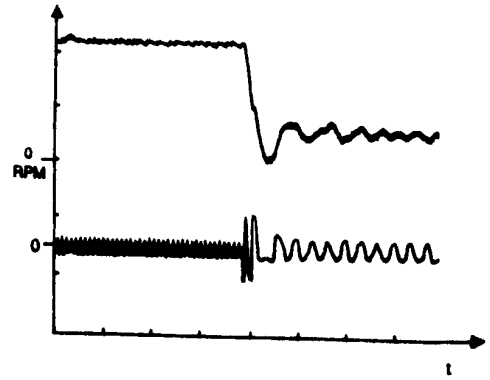

Fig. 18: Respose to step in speed command from 600 to 120 rpm at no load. Top trace: Speed (226 rpm/div). Bottom trace: Current (10 amp/ div). Time scale: 500 ms/div.

CONCLUSION

An implementation for a low cost direct field oriented drive that makes use of tapped stator windings as flux sensors has been presented. The major advantages are due to the simple design of the flux loop controller starting from the derivative of the airgap flux and elimination of any need to compensate for stator IR drop. The use of rotor slot ripple for mechanical speed detection has been shown to be an effective method of regulating speed without a tachometer.

ACKNOWLEDGMENTS

The work reported in this paper was made possible by support from the industrial sponsors of the Wisconsin Electric Machines and Power Electronics Consortium (WEMPEC) to whom the authors are greatly indebted. The authors would like to give special recognition to Mr. Gary Peterson, of Marathon Electric Co. for constructing the experimental machine.

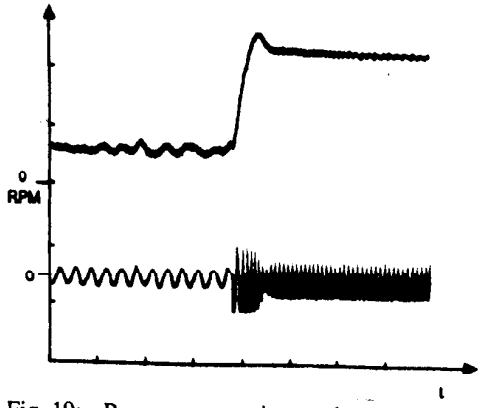

Fig. 19: Respose to step in speed command from 120 to 600 rpm with load proportional to speed and 0.5 pu torque at 600 rpm. Top trace: Speed (226 rpm/div). Bottom trace: Current (10 amp/div). Time scale: 500 ms/div.

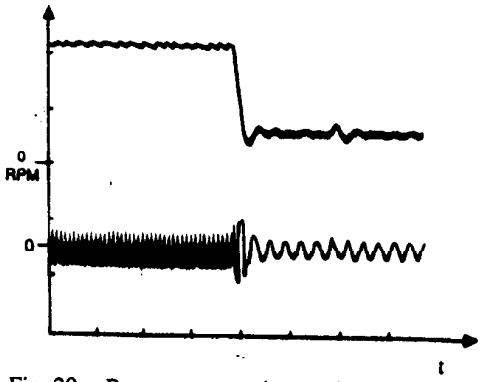

Fig. 20: Respose to step in speed command from 600 to 120 rpm with load proportional to speed and 0.5 pu. torque at 600 rpm. Top trace: Speed (226 rpm/div). Bottom trace: Current (10 amp/div). Time scale: 500 ms/div.

REFERENCES

[1] T.A. Lipo and K.C. Chang,"A New Approach to Flux and Torque Sensing in Induction Machines", *IEEE Trans. on Industry Applications*, vol. IA-22, July/August 1986, pp. 731-737.

[2] F.Profumo, D. Zinger, T.A.Lipo,"Design of a Robust Controller for Direct Field Oriented Control of an Induction Motor", Electrical Drives Symposium, Cagliari, Italy, Sept. 1987, pp. 137-143.

[3] T. A. Lipo and M. S. Kramer,"Measurement of Induction Motor Torque Pulsations Due to Inverter Supply," *Electrical Noise in Electrical Machines*, Elsevier Press (book) (To appear).

[4] M. Ishida, K. Iwata,"New Slip Frequency Detector of an Induction Motor Utilizing Rotor Slot Harmonics", Proceedings of International Semiconductor Power Conference, Orlando, Fl., May 1982, pp. 408-415.

[5] P.L. Alger, *Induction Machines*, (New York:Gordon and Beach,1970) pp. 377-382

[6] B.J. Hosticka, R.W. Broderson, and P.R. Gray,"MOS Sampled Data Recursive Filters Using Switched Capacitor Integrators," *IEEE Journal of Solid State Circuits*, Vol. SC-12 No. 6, Dec 1977, pp 600-608.

[7] R.Gardner, *Phase Locked Loop Techniques* (John Wiley and Sons, 1966)